The Astrophysical Journal Letters, 826:L27 (6pp), 2016 August 1 doi:10.3847/2041-8205/826/2/L27

DDO 68: A FLEA WITH SMALLER FLEAS THAT PREY ON HIM

Francesca Annibali[1,2], Carlo Nipoti[2], Luca Ciotti[2], Monica Tosi[1], Alessandra Aloisi[3], Michele Bellazzini[1], Michele Cignoni[4], Felice Cusano[1], Diego Paris[5], and Elena Sacchi[1,2]
[1] INAF–Bologna Observatory, via Ranzani 1, I-40127 Bologna, Italy
[2] Department of Physics and Astronomy, University of Bologna, viale Berti-Pichat 6/2, I-40127 Bologna, Italy
[3] Space Telescope Science Institute, 3700 San Martin Drive, Baltimore, MD 21218, USA
[4] Physics Department, University of Pisa, Largo Bruno Pontecorvo 3, I-56127 Pisa, Italy
[5] INAF-Rome Observatory, Via Frascati 33, I-00078 Monte Porzio, Italy
Received 2016 June 16; revised 2016 July 7; accepted 2016 July 8; published 2016 July 29

ABSTRACT

We present new photometry of the dwarf irregular galaxy DDO 68, one of the most metal-poor and least massive dwarfs, located in the Lynx-Cancer Void. The images were acquired with the Large Binocular Telescope in the g and r passbands and show unequivocally that DDO 68 has previously unknown stellar streams related to the accretion of at least two smaller companions: *a flea with smaller fleas biting it*, to put it in Jonathan Swift's words (from Jonathan Swift's *On Poetry: a Rhapsody*: So, naturalists observe, a flea/has smaller fleas that on him prey/and these have smaller still to bite em/and so proceed ad infinitum). Our data provide direct observational evidence of multiple galaxy merging occurring at very low galactic mass scales. We present the results of an *N*-body simulation of the interaction of three dwarf galaxies that reproduce well the main morphological features of DDO 68.

Key words: galaxies: dwarf – galaxies: formation – galaxies: individual (DDO 68) – galaxies: interactions – galaxies: irregular – galaxies: kinematics and dynamics

1. INTRODUCTION

In Lambda cold dark matter cosmology, galaxies grow continuously in mass through hierarchical assembly of smaller systems (e.g., White & Rees 1978; Diemand et al. 2008), and dark matter halos host substructures down to the resolution limit of the simulations (Diemand et al. 2008; Wheeler et al. 2015). Observationally, there is ample evidence of accretion of satellites onto massive galaxies such as the Milky Way, Andromeda, several Local Volume spirals, and the giant elliptical Centaurus A (see, e.g., Ibata et al. 2001; Belokurov et al. 2006; McConnachie et al. 2009; Martinez-Delgado et al. 2010; Crnojevic et al. 2016). Yet, evidence of stellar streams around dwarf galaxies is currently limited (Martinez-Delgado et al. 2012; Rich et al. 2012; Belokurov & Koposov 2016); in particular, no clear cut stellar stream has been detected so far around galaxies less massive in stars than $10^9\,M_\odot$, except for a kinematical signature suggesting that the dwarf satellite of M31—And II—ingested a smaller system in the past (Amorisco et al. 2014).

DDO 68 is a star-forming dwarf galaxy located in the Lynx-Cancer void (Pustilnik & Tepliakova 2011) at a distance of $\simeq$12.7 Mpc from the Earth (Cannon et al. 2014; Sacchi et al. 2016). With an oxygen abundance (Pustilnik et al. 2005; Izotov & Thuan 2009) about 1/40 of solar (Caffau et al. 2008), it is one of the most metal-poor star-forming dwarfs known so far, much more metal-poor than typical dwarfs of a similar mass (Pustilnik et al. 2005). It also exhibits a very distorted morphology, with a cometary tail (hereafter the Tail) populated by stars of all ages (Tikhonov et al. 2014; Sacchi et al. 2016) and particularly rich in H II regions, that extends from the main body of the galaxy for a projected length of $\simeq$5 kpc. Because of these peculiar properties, DDO 68 has already been suggested to be affected by galaxy interaction (Ekta et al. 2008; Cannon et al. 2014; Tikhonov et al. 2014), although with no conclusive evidence. Ekta et al. noticed distortions in the H I distribution and interpreted the observed features in terms of a late-stage merger of two gas-rich progenitors. Tikhonov et al. proposed that the Tail is actually a disrupted satellite (dubbed DDO 68 B) being currently accreted by DDO 68, while Cannon et al. identified a possible H I satellite (DDO 68 C), with $M_{\rm H\,I} \simeq 3 \times 10^7\,M_\odot$, at a projected distance of $\simeq$40 kpc from the main body.

We studied DDO 68 with deep images acquired with the Advanced Camera for Surveys (ACS) on board the *Hubble Space Telescope* (*HST*; GO 11578, PI: Aloisi). With those data, we (Sacchi et al. 2016) resolved its stellar content, characterized its star formation history (SFH) with the synthetic color–magnitude diagram (CMD) method (Tolstoy et al. 2009; Cignoni & Tosi 2010), and constrained its distance via the tip of the red giant branch (RGB) and the synthetic CMDs. From the resulting SFH, we inferred that the total mass in stars ever formed in the system is only $1.2 \times 10^8\,M_\odot$. DDO 68 is of special interest as a possible accretor because of this low mass, which puts it close to the resolution limit of galaxy formation models.

The ACS field of view is too small to look for satellites or streams around the galaxy. To obtain very deep imaging that could reveal the presence of previously unknown faint stellar substructures connected to DDO 68, we exploited the perfect combination of large field of view and excellent photometric depth of the LBT Large Binocular Camera (LBC) covering a large area around our target. In this Letter, we report the successful results obtained from the LBT photometry, with clear evidence that, in addition to the Tail and DDO 68 C, the system also hosts an independent small stream and several arc-like structures. To better interpret the LBT data in terms of the dynamical status of the system, we have also run *N*-body simulations and found that the observed configuration is consistent with the presence of at least two different satellites being accreted by the galaxy main body.

2. LBT PHOTOMETRY

We observed DDO 68 with LBT in 2016 January 12 and 13, with the wide-field ($\simeq$23 arcmin × 23 arcmin) LBC cameras

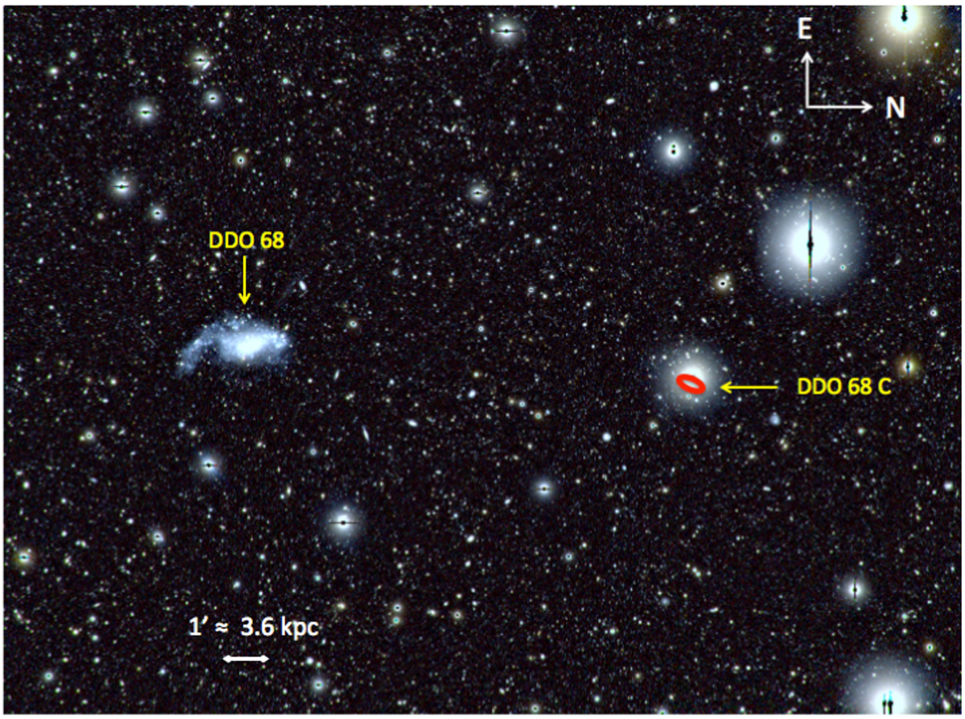

Figure 1. Deep LBC g and r color-combined image of DDO 68. The positions of DDO 68 and of the candidate H I companion DDO 68 C are indicated. DDO 68 C is masked by a bright foreground star, but we have drawn its spatial extension (red ellipse) as detected in the ultraviolet *GALEX* images. The total displayed field of view is ≃0.4 × 0.3 square degrees, corresponding to ≃90 × 70 kpc^2 at DDO 68's distance of ≃12.7 Mpc.

operated in binocular mode. Images in the Sloan Digital Sky Survey (SDSS) g and r passbands were obtained with the LBC-blue and LBC-red cameras, respectively. The total exposure time of ≃2 hr in each band was organized into 5 visits of 180 s times 8 dithered exposures. For a straightforward calibration into the SDSS photometric systems, we also acquired in each band 4 short exposures of 30 s each to serve for the photometry of bright foreground stars in common with the SDSS catalog. With our exposures, we reached a surface-brightness limit of $\mu \simeq 29$ mag arcsec^{-2} in the g and r bands.

The reduction of the g- and r- LBC images was performed with the pipeline developed at INAF-OAR (D. Paris et al. 2016, in preparation). The individual raw images were first corrected for bias and flat field and then were background-subtracted. After astrometric calibration, they were combined into g- and r-band stacked images with the SWarp software (Bertin et al. 2002).

Our color-combined LBT image is displayed in Figure 1, where both DDO 68 and the position of the candidate companion DDO 68 C (Cannon et al. 2014) are indicated. The new substructures/satellites discovered here are much closer to the main body of DDO 68 and are visible in Figure 2, where blow-ups of some portions of the whole image are displayed. Remarkably, Figure 2, besides the already well-known Tail, reveals several previously undetected faint stellar substructures. The most prominent of these are an arc embracing the western side of DDO 68 for a projected extension of ≃5 kpc (hereafter the Arc) and a stream (which we dub DDO 68-S1, i.e., Stream 1) as faint as $\mu_r \simeq 28.7$ mag arcsec^{-2} that extends for ≃4.6 kpc along the NE–SW direction (the system at the NE end of S1 is most likely a background spiral galaxy). While S1 is well detected in both the g and r images, the Arc is mostly visible in g, due to the presence of younger stars than in S1 (see Section 3).

The total magnitude of S1 in the r band was derived within the region drawn in Figure 3 using the *polyphot* task in the *apphot* IRAF[6] package. The background was evaluated drawing the same area in regions randomly placed around S1 avoiding both DDO 68 and bright foreground stars, and performing photometry in the same way as for S1. This procedure allowed us to remove the contribution from both the sky and the background galaxies. The average (g–r) color was instead computed performing photometry within a few small (2 arcsec in radius) circular apertures selected in regions of S1 free of visible contaminants (see Figure 3(a)), with the background evaluated in similar apertures placed in free regions around S1. Finally, the calibration of the instrumental magnitudes into the SDSS system was accomplished through photometry on our short exposures of stars cataloged in the SDSS.

We obtain a total integrated magnitude for S1 of $m_{r,S1} = 21.6 \pm 0.4$ and average color of $(g–r)_{S1} = 0.56 \pm 0.11$, computed within an area of ≃700 arcsec^2. This provides an average surface brightness $\mu_{r,S1} \simeq 28.7$ mag arcsec^{-2}. Adopting a distance of 12.7 Mpc (Sacchi et al. 2016), or $(m–M)_0 \simeq 30.5$, and a foreground reddening of $E(B-V) = 0.018$ (Schlegel et al. 1998), we derive an absolute intrinsic magnitude $M_{r,S1} = -9.0 \pm 0.4$ and an intrinsic color $(g–r)_{0,S1} = 0.54 \pm 0.11$.

3. PHYSICAL PROPERTIES OF THE SUBSTRUCTURES

Both the Arc and a small portion of S1 fall into our ACS@HST images and are resolved into individual stars. Their CMDs (see Figure 4) host RGB stars with luminosities

[6] IRAF is distributed by the National Optical Astronomy Observatory, operated by AURA.

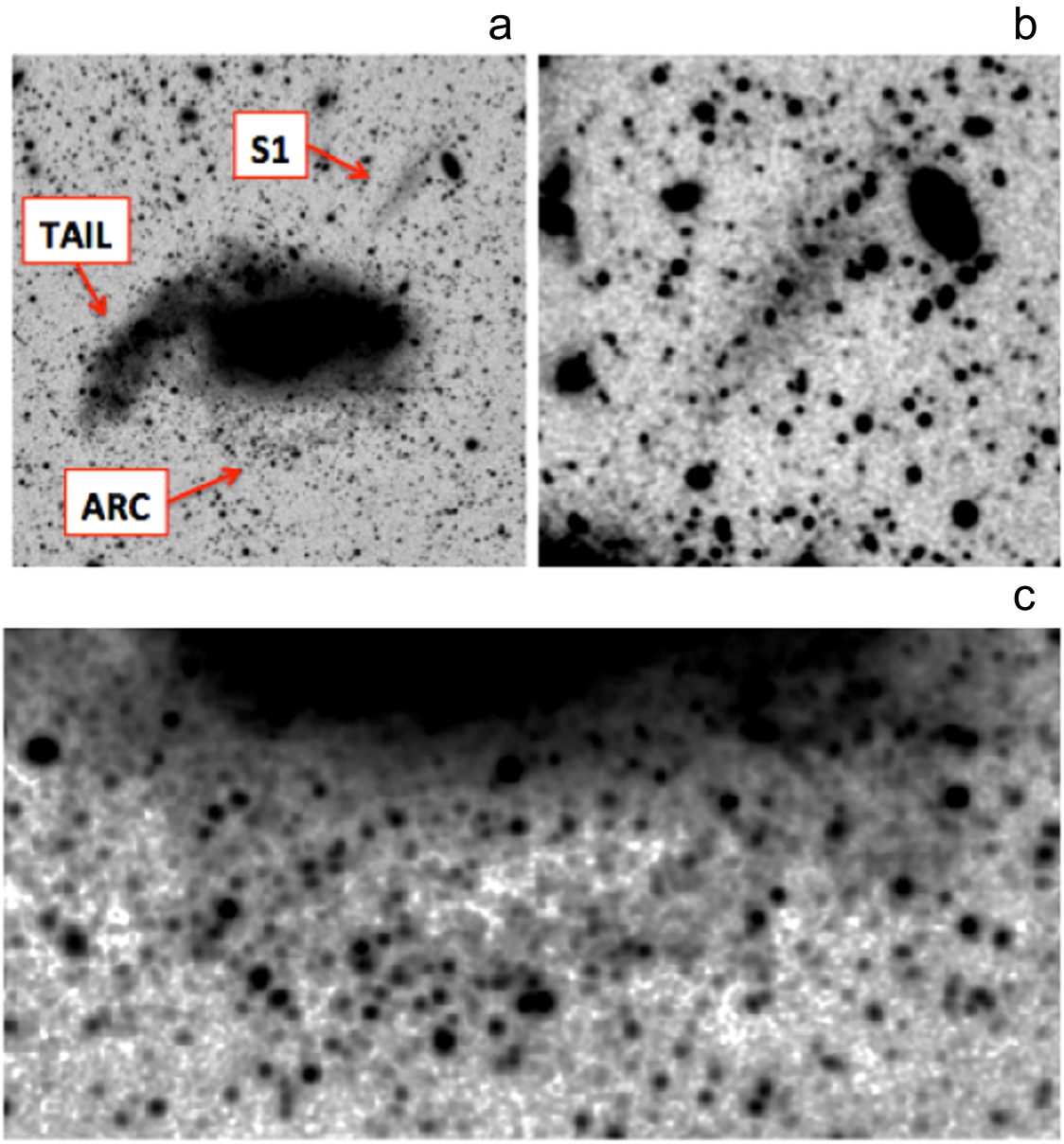

Figure 2. Blow-ups of key portions of the LBT image of DDO 68. (a) Portion of the g-band image (FoV $\simeq$ 280 $\times$ 280 arcsec^2, or 17 $\times$ 17 kpc^2) showing the Tail, Arc, and Stream S1. A Gaussian smoothing has been applied to the image to better highlight low surface-brightness features. (b) Further blow-up (FoV $\simeq$ 90 $\times$ 90 arcsec^2, or 5 $\times$ 5 kpc^2) in the r band showing S1 in detail. (c) Blow-up of panel (a) (FoV $\simeq$ 140 $\times$ 60 arcsec^2, or 8.4 $\times$ 3.6 kpc^2) in the g band showing the Arc in detail.

compatible with DDO 68's distance. This indicates that both structures are physically associated with DDO 68.

The CMD of the Arc implies a wide range of ages, with most of the measured stars $\simeq$200–300 Myr old, a few as young as 50 Myr, and several RGB stars older than 2 Gyr and possibly up to 13 Gyr old. Unfortunately, the age–metallicity degeneracy of the RGB colors, coupled with the large photometric errors, prevents us from safely distinguishing a 2 Gyr old from a 13 Gyr old population in DDO 68.

The resolved portion of S1 exhibits a population older than the Arc since its CMD is only populated by RGB stars, with ages $\gtrsim$2 Gyr. To further characterize S1's stellar population, we compared its intrinsic color derived in the previous section with the PARSEC v1.2S + COLIBRI PR16 simple stellar population (SSP) models (Bressan et al. 2012; Marigo et al. 2013; Rosenfield et al. 2013), for a Kroupa initial mass function (IMF; Kroupa 2001), at DDO 68' s metallicity of $Z = 0.0004$ ($\simeq 1/40$ of solar, where $Z_\odot = 0.0152$) and at a lower metallicity of $Z = 0.0001$ ($\simeq 1/150$ solar). The S1 color implies, within a 1σ error, a population older than 5 Gyr, and possibly as old as the age of the universe (Figure 3(b)). This is in agreement with the fact that the portion of S1 sampled by our *HST* data is resolved into RGB stars (Figure 4), which can have ages in the range 2–13 Gyr. From the SSP models, we derive a total S1 luminosity of $\simeq 3.5 \times 10^5\, L_\odot$. To derive a stellar mass range for S1, we conservatively adopted two age extremes at 2 and 13 Gyr, which provide a current stellar mass in the range (1.5–6) $\times 10^5\, M_\odot$. S1 is then comparable to the ultra-faint

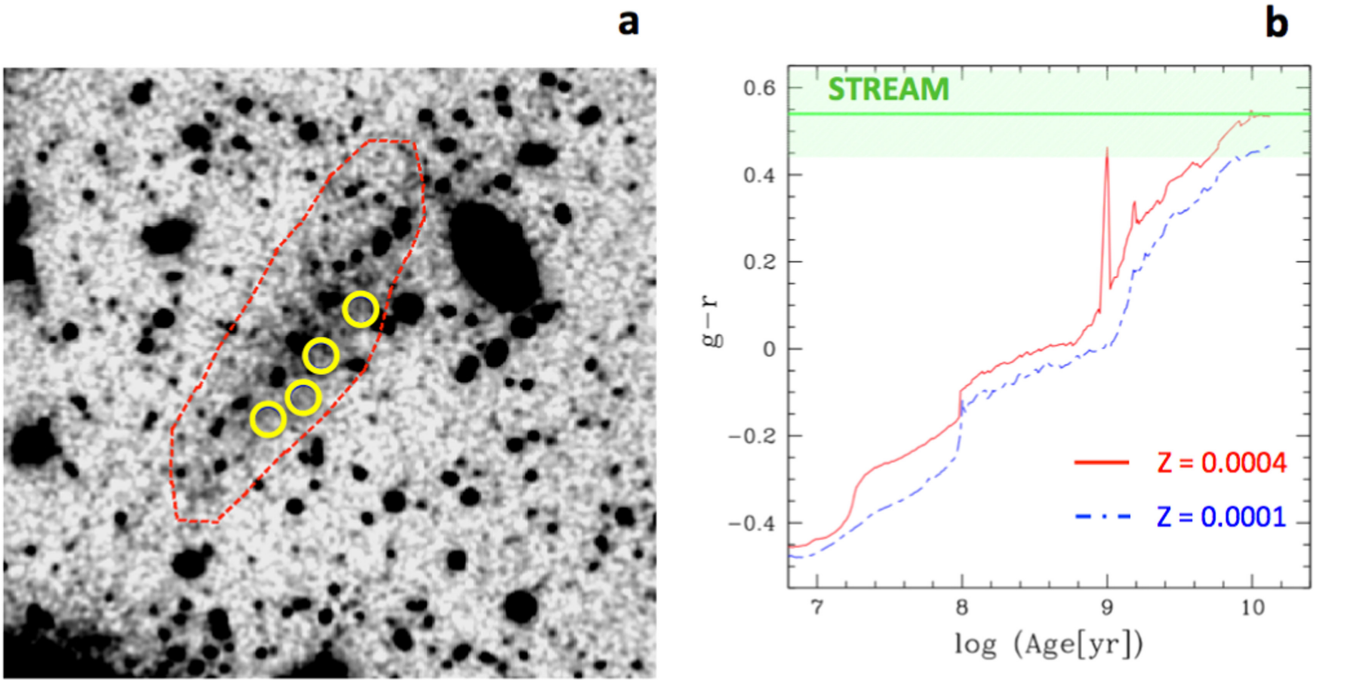

Figure 3. (a) LBT r-image of the stream DDO 68-S1 (FoV $\simeq 90 \times 90$ arcsec^2) overlaid with both the region (red dashed line) selected to compute its total magnitude and the circular apertures, free of visible contaminating galaxies, selected to compute its color. (b) g–r color of SSP models as a function of age. The plotted models are the PARSEC ones for the two metallicities $Z = 0.0001$ and 0.0004 and a Kroupa IMF. The green horizontal line and the shaded area indicate the intrinsic $(g–r)_0$ color of S1 and its $\pm 1\sigma$ uncertainty.

satellites of the Milky Way (Belokurov et al. 2007, 2010), although it may also be just a portion of a larger disrupted progenitor.

The significantly different stellar populations of the Arc and S1 suggest that the two substructures originated from two different systems.

4. DYNAMICS OF DDO 68

A possible interpretation of the morphology of DDO 68 is that the Tail, the Arc, and S1 are tidal features due to the stripping effect of a passing body. However, no nearby objects in the direction of the Tail, the Arc, or S1 are detected in Figure 1 or in the SDSS images. A simple estimate of the mass M_p of a putative perturber at distance d from the main body of DDO 68 is given by the fact that a significant stripping can be produced only for $M_p \simeq M_{tot} d^3/R^3$, where M_{tot} is the total mass and R is a fiducial radius of DDO 68. This leads us to deduce implausibly high values for the mass of an otherwise undetected perturber. For example, the minimum mass of a perturber located at a distance d three times the length of the Tail ($R \simeq 5$ kpc) would be $M_p \simeq 30\, M_{tot}$. This argument excludes that the Tail, the Arc, and S1 are tidal features due to DDO 68 C, which is at a distance of 42 kpc (Cannon et al. 2014) from the main body and has a baryonic mass $\approx$10 times smaller than that of DDO 68.

Being that tidal stripping is excluded as the cause of the three non-equilibrium features, the alternative is that they are due to the accretion of smaller companions. Support for the interpretation of DDO 68 as an ongoing multiple merger comes from the results of N-body simulations. We ran several simulations of possible merging events in DDO 68 with the parallel collisionless N-body code FVFPS (Nipoti et al. 2003). For simplicity, we include only the collisionless component (stars and dark matter) in the simulations, and we do not model the physics of the gas. We found that while the Tail and a structure similar to the Arc are reproduced by the accretion of a 10 times less massive satellite galaxy (with the Tail surviving for $\simeq$100 Myr and consisting mainly of stars of the satellite), the formation of S1 requires an additional accreting system. We thus performed simulations (see the Appendix for details) in which the main galaxy of mass M_{tot} interacts simultaneously with two smaller satellites, named T and S, of mass $M_{tot}/10$ and $M_{tot}/150$, respectively. As an example, we compare in Figure 5 the LBT image of DDO 68 with a snapshot of one of these N-body simulations that reproduces well all its main morphological features. In this snapshot, the spatial distributions of the stars of satellites T and S correspond, respectively, to the Tail and to S1.

5. CONCLUSIONS

Our study of DDO 68 shows clear evidence of stellar streams around a galaxy with stellar mass as low as $M_{star} \simeq 10^8$ $M_\odot$ and located in a void. DDO 68 is an extremely isolated system and yet it appears surrounded by smaller, interacting bodies: the Tail (or DDO 68 B, in the notation of Tikhonov et al. 2014), DDO 68 C (discovered by Cannon et al. 2014), the Arc, and S1, detected now with LBT.

A simple dynamical analysis suggests that the observed morphological features (Tail, Arc, and S1) are not the effect of tidal interaction with massive companions, but are instead the signature of an ongoing multiple merging, as confirmed by our N-body simulations. The simulation, which is admittedly simplified, must be considered only an illustrative case and not necessarily the best possible way to reproduce the complex morphology of DDO 68.

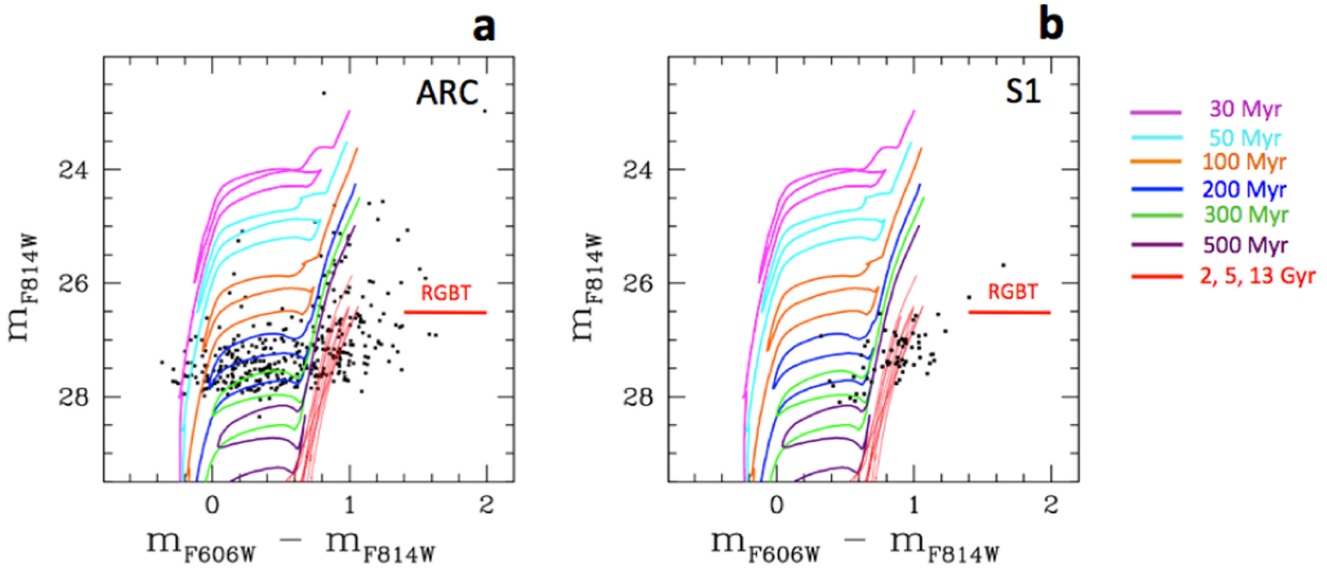

Figure 4. *HST* color–magnitude diagrams of the Arc and of S1 in DDO 68. (a) CMD of the stars resolved in our ACS@HST images that belong to the region outlined by the Arc. Superimposed are the PARSEC isochrones (Bressan et al. 2012) for a metallicity $Z = 0.0004$ and for different ages, shifted according to DDO 68's distance and foreground reddening. The horizontal segment indicates the location of the tip of the red giant branch as derived by Sacchi et al. (2016). (b) Same as panel (a), but for the small portion of S1 falling within the *HST* images. S1 is mainly populated by RGB stars, implying ages older than 2 Gyr.

Multiple accretions of dwarf systems onto a more massive host are expected from observations showing that dwarfs are often found in associations (see, e.g., Tully et al. 2006; Bellazzini et al. 2013) and from cosmological simulations predicting that sub-halos are often accreted in small groups (Li & Helmi 2008)—a scenario that could explain the association of some Milky Way dwarfs with the plane of the orbit of the Magellanic Clouds (D' Onghia & Lake 2008). In DDO 68, we are witnessing multiple accretions of smaller systems in action. We suggest that it is not just a coincidence that these *fleas of fleas* are so clearly observed for the first time in such an isolated system: once a group of dwarfs with their satellites falls into a massive host, like the Milky Way, it is eventually disassembled by tidal forces wiping out evidence of coherent structure (Deason et al. 2015; Wheeler et al. 2015). It is natural to expect satellites of satellites residing in small halos, i.e., in lower-density environments, to survive longer than those residing in more massive halos.

While all dwarf irregulars show distorted morphologies, by definition, this does not imply that these are produced by recent merging events. Here, we have identified very specific signatures (like, e.g., a stream made of old stars that cannot originate from internal hydrodynamical processes) that are not usually seen in other dIrrs. Yet, lack of evidence is not evidence of lack and might instead be due to insufficient sensitivity of the available observations. Our result demonstrates the potential of wide-field instrumentation at 8–10 m telescopes to search for substructures around dwarfs.

We thank V. Belokurov for the nice review. This Letter is based on LBT images acquired within the Italian Director Discretionary Time, for which we are grateful. We acknowledge support from the LBT-Italian Coordination Facility and the Italian LBT Spectroscopic Reduction Center for the execution of observations, data distribution, and reduction. F.A. was partially funded through the Italian PRIN-MIUR 2010LY5N2T-006.

APPENDIX
N-BODY SIMULATION

In the initial conditions of the *N*-body simulation shown in Figure 5(b), the main galaxy is represented by an equilibrium spherical isotropic dark matter halo and a stellar disk. The halo has $\gamma = 0$ density profile (Dehnen 1993) $\rho(r) \propto (r + a)^{-4}$ with scale radius $a = 4$ kpc and total mass $1.3 \times 10^{10}\,M_{\odot}$ (the mass within 11 kpc is $5.3 \times 10^{9}\,M_{\odot}$, consistent with the observational estimate of the dynamical mass of DDO 68; Cannon et al. 2014). The stellar disk is assumed to be razor thin, with exponential surface density profile $\Sigma(R) \propto \exp(-R/R_{*})$ with $R_{*} = 1.02$ kpc. This profile provides a satisfactory fit to the completeness-corrected stellar counts as a function of radius as derived from the *HST* photometry. In the simulation, the stellar particles are in circular orbits in the gravitational potential of the halo. The gravitational potential of the stars is neglected, which is justified because the dynamical mass is about 20 times the stellar mass within a radius of 11 kpc for DDO 68.

The satellites are scaled-down versions of the same model used for the main galaxy (spherical $\gamma = 0$ halo and thin exponential stellar disk). Satellite T has halo scale radius $a = 1.86$ kpc, total mass $1.3 \times 10^{9}\,M_{\odot}$, and stellar scale radius $R_{*} = 0.47$. Satellite S has halo scale radius $a = 1.2$ kpc, total mass $8.6 \times 10^{7}\,M_{\odot}$, and stellar scale radius $R_{*} = 0.3$ kpc. As for the main galaxy, the stellar particles of the satellites also are just tracers: their gravitational potential is neglected. The number of dark matter particles is 3×10^{5} for the main galaxy, 3×10^{4} for satellite T, and 2×10^{3} for satellite S. In each system, the stellar disk is represented with the same number of particles used for the dark matter halo.

Taking a Cartesian coordinate system with the origin in the center of mass of the main galaxy, the initial ($t = 0$) center-of-mass positions and velocities are $x = 10$ kpc, $v_{y} = -45$ km s^{-1}, and $y = z = v_{x} = v_{z} = 0$ for satellite T and $x = -10$ kpc, $y = 4.37$ kpc, $v_{z} = 45$ km s^{-1}, and $z = v_{x} = v_{y} = 0$ for satellite S (both satellites are approximately in circular orbit in the

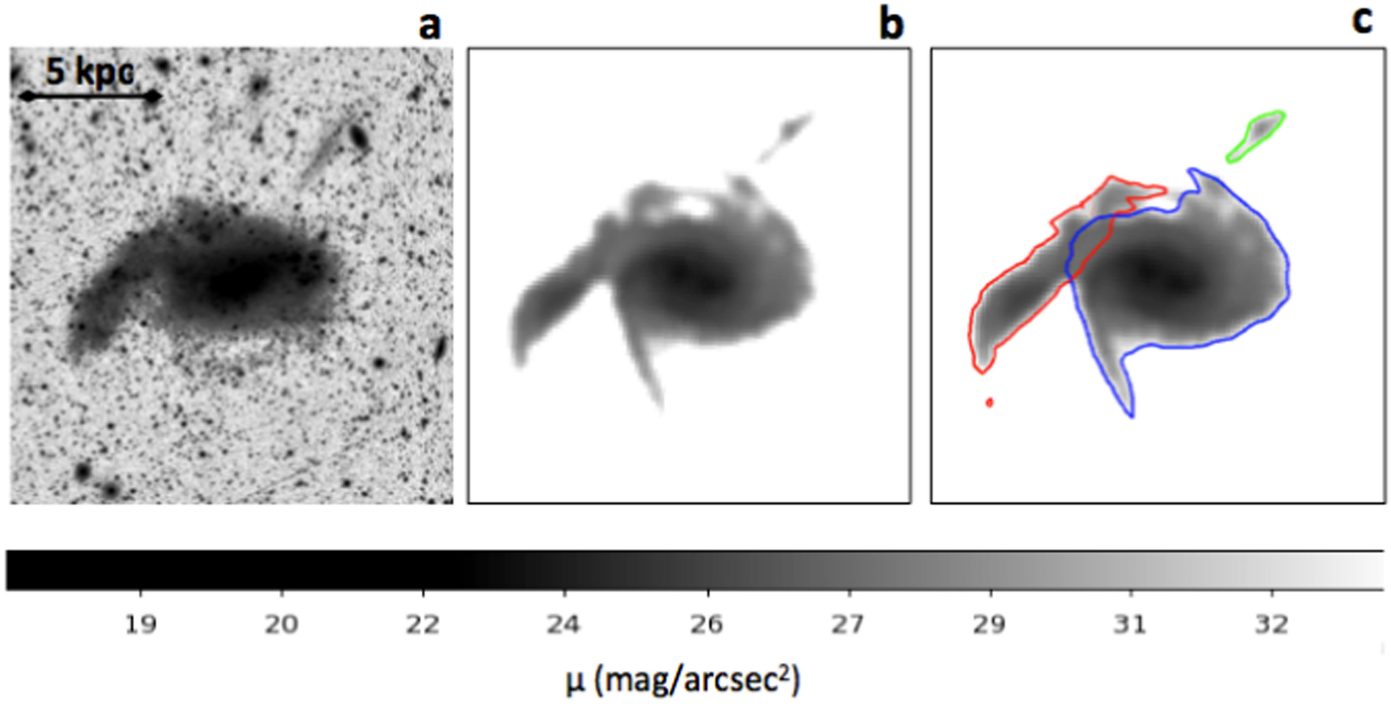

Figure 5. (a) g-band image of DDO 68 in surface-brightness scale. (b) Snapshot of the stellar component of the multiple-merger *N*-body simulation. The observed and the simulated images are displayed on the same spatial and surface-brightness scales. We note that elongated arc-like substructures, akin to the observed Arc (see Figure 2(a)), are present in the mock image. (c) Final snapshot of the *N*-body simulation with superimposed contours delimiting the regions whose bulk stars originally belong to the main galaxy (blue), to satellite T (red), and to satellite S (green).

gravitational potential of the main galaxy). The orientation of this Cartesian system is such that the y axis lies in the plane of the main galaxy disk, which forms an angle of 45° with the x axis. The disk of satellite T lies in the satellite's orbital plane, while the disk of satellite S is orthogonal to the satellite's orbital plane. In the simulation, the evolution of the system is followed for 1 Gyr. The time step, which is allowed to vary with time as a function of the maximum mass density (Nipoti et al. 2003), is typically in the range 1–2 Myr. The softening length is 30 pc. The snapshot shown in Figure 5(b) is obtained at $t = 630$ Myr assuming a line of sight such that the disk of the main galaxy at $t = 0$ has an inclination of 60°.

REFERENCES

Amorisco, N. C., Evans, N. W., & van de Ven, G. 2014, Natur, 507, 335
Bellazzini, M., Oosterloo, T., Fraternali, F., & Beccari, G. 2013, A&A, 559, L11
Belokurov, V., & Koposov, S. E. 2016, MNRAS, 456, 602
Belokurov, V., Zucker, D. B., Evans, N. W., et al. 2006, ApJL, 642, L137
Belokurov, V., Zucker, D. B., Evans, N. W., et al. 2007, ApJ, 654, 897
Belokurov, V., Zucker, D. B., Evans, N. W., et al. 2010, ApJL, 712, L103
Bertin, E., Mellier, Y., Radovich, M., et al. 2002, in ASP Conf. Proc. 281, Astronomical Data Analysis Software and Systems XI, ed. D. A. Bohlender, D. Durand, & T. H. Handley (San Francisco, CA: ASP), 228
Bressan, A., Marigo, P., Girardi, L., et al. 2012, MNRAS, 27, 127
Caffau, E., Ludwig, H.-G., Steffen, M., et al. 2008, A&A, 488, 1031
Cannon, J. M., Johnson, M., McQuinn, K. B., et al. 2014, ApJL, 787, L1
Cignoni, M., & Tosi, M. 2010, AdAst, 2010, 158568
Crnojevic, D., Sand, D. J., Spekkens, K., et al. 2016, ApJ, 823, 19
Deason, A. J., Wetzel, A. R., Garrison-Kimmel, S., & Belokurov, V. 2015, MNRAS, 453, 3568
Dehnen, W. 1993, MNRAS, 265, 250
Diemand, J., Kuhlen, M., Madau, P., et al. 2008, Natur, 454, 735
D' Onghia, E., & Lake 2008, ApJL, 686, L61
Ekta, Chengalur, J. N., & Pustilnik, S. A. 2008, MNRAS, 391, 881
Ibata, R., Irwin, M., Lewis, G., Ferguson, A. M. N., & Tanvir, N. 2001, Natur, 412, 49
Izotov, Y. I., & Thuan, T. X. 2009, ApJ, 690, 1797
Kroupa, P. 2001, MNRAS, 322, 231
Li, Y. S., & Helmi, A. 2008, MNRAS, 385, 1365
Marigo, P., Bressan, A., Nanni, A., Girardi, L., & Pumo, M. L. 2013, MNRAS, 434, 488
Martinez-Delgado, D., Gabany, R. J., Crawford, K., et al. 2010, AJ, 140, 962
Martinez-Delgado, D., Romanowsky, A. J., Gabany, R. J., et al. 2012, ApJL, 748, L24
McConnachie, A. W., Irwin, M. J., Ibata, R. A., et al. 2009, Natur, 461, 66
Nipoti, C., Londrillo, P., & Ciotti, L. 2003, MNRAS, 342, 501
Pustilnik, S. A., Kniazev, A. Y., & Pramskij, A. G. 2005, A&A, 443, 91
Pustilnik, S. A., & Tepliakova, A. L. 2011, MNRAS, 415, 1188
Rich, R. M., Collins, M. L. M., Black, C. M., et al. 2012, Natur, 482, 192
Rosenfield, P., Girardi, L., Dalcanton, J., et al. 2013, BAAS, 221, 213.06
Sacchi, E., Annibali, F., Cignoni, M., et al. 2016, ApJ, in press (arXiv:1604.06239)
Schlegel, D. J., Finkbeiner, D. P., & Davis, M. 1998, ApJ, 500, 525
Tikhonov, N. A., Galazutdinova, O. A., & Lebedev, V. S. 2014, AstL, 40, 1
Tolstoy, E., Hill, V., & Tosi, M. 2009, ARA&A, 47, 371
Tully, R. B., Rizzi, L., Dolphin, A. E., et al. 2006, AJ, 132, 729
Wheeler, C., Oñorbe, J., Bullock, J. S., et al. 2015, MNRAS, 453, 1305
White, S. D. M., & Rees, M. J. 1978, MNRAS, 183, 341